

14. Lozovik Yu E, Berman O L *Pis'ma Zh. Eksp. Teor. Fiz.* **64** 526 (1996) [*JETP Lett.* **64** 573 (1996)]; *Zh. Eksp. Teor. Fiz.* **111** 1879 (1997) [*JETP* **84** 1027 (1997)]; Lozovik Yu E, Berman O L, Ruvinskii A M *Pis'ma Zh. Eksp. Teor. Fiz.* **69** 573 (1999) [*JETP Lett.* **69** 616 (1999)]
15. Lozovik Yu E, Yudson V I *Solid State Commun.* **22** 117 (1977); Klyuchnik A V, Lozovik Yu E *J. Phys. C: Solid State Phys.* **11** L483 (1978); Lozovik Yu E, Klyuchnik A V *J. Phys. Low Temp.* **38** 761 (1980); Shevchenko S I *Phys. Rev. Lett.* **72** 3242 (1994); Lozovik Yu E, Poushnov A V *Phys. Lett. A* **228** 399 (1997)
16. Keldysh L V, in *Electron-Hole Liquid* (Amsterdam: North-Holland, 1986)
17. Keldysh L V, Kopaev Yu V *Fiz. Tver. Tela* **6** 2791 (1964) [*Sov. Phys. Solid State* **6** 2219 (1965)]
18. Kozlov A N, Maksimov L A *Zh. Eksp. Teor. Fiz.* **48** 1184 (1965) [*Sov. Phys. JETP* **21** 790 (1965)]; Halperin B I, Rice T M *Solid State Phys.* **21** 115 (1968); Guseinov R R, Keldysh L V *Zh. Eksp. Teor. Fiz.* **63** 2255 (1972) [*Sov. Phys. JETP* **36** 1193 (1973)]
19. Lozovik Yu E, Merkulova S P, Sokolik A A *Usp. Fiz. Nauk* **178** 757 (2008) [*Phys. Usp.* **51** 727 (2008)]; Lozovik Yu E, Sokolik A A *Pis'ma Zh. Eksp. Teor. Fiz.* **87** 61 (2008) [*JETP Lett.* **87** 55 (2008)]
20. Berman O L, Lozovik Yu E, Gumbs G *Phys. Rev. B* **77** 155433 (2008)
21. Lozovik Yu E, Poushnov A V *Phys. Rev. B* **58** 6608 (1998); Lozovik Yu E, Pushnov A V *Zh. Eksp. Teor. Fiz.* **115** 1353 (1999) [*JETP* **88** 747 (1999)]; Lozovik Yu E, Ovchinnikov I V *Phys. Rev. B* **66** 075124 (2002); Lozovik Yu E, Kurbakov I L, Ovchinnikov I V *Solid State Commun.* **126** 269 (2003); Lozovik Yu E, Ovchinnikov I V, Sharapov V A *Zh. Eksp. Teor. Fiz.* **125** 659 (2004) [*JETP* **98** 582 (2004)]
22. Balili R B et al. *Appl. Phys. Lett.* **88** 031110 (2006); Berman O L, Lozovik Yu E, Snoke D W *Phys. Status Solidi C* **3** 3373 (2006)
23. Gorbunov A V, Timofeev V B *Usp. Fiz. Nauk* **176** 651 (2006) [*Phys. Usp.* **49** 629 (2006)]; Timofeev V B, Gorbunov A V *Pis'ma Zh. Eksp. Teor. Fiz.* **83** 178 (2006) [*JETP Lett.* **83** 146 (2006)]
24. Butov L V *J. Phys. Condens. Matter* **19** 295202 (2007)
25. Lozovik Yu E, Kurbakov I L, Willander M *Phys. Lett. A* **366** 487 (2007)
26. Lozovik Yu E, Berman O L *Phys. Scripta* **58** 86 (1998); Kulakovskii D V, Lozovik Yu E, Chaplik A V *Zh. Eksp. Teor. Fiz.* **126** 979 (2004) [*JETP* **99** 850 (2004)]
27. Astrakharchik G E, Boronat J, Kurbakov I L, Lozovik Yu E *Phys. Rev. Lett.* **98** 060405 (2007); Ludwig P, Filinov A, Lozovik Yu E, Stolz H, Bonitz M *Contrib. Plasma Phys.* **47** 335 (2007)
28. Lozovik Yu E et al. *Zh. Eksp. Teor. Fiz.* **133** 348 (2008) [*JETP* **106** 296 (2008)]; Astrakharchik G E et al. *Phys. Rev. A* **75** 063630 (2007)
29. Vörös Z et al. *Phys. Rev. Lett.* **97** 016803 (2006)
30. Lozovik Yu E, Ruvinsky A M *Phys. Lett. A* **227** 271 (1997); Lozovik Yu E et al. *Phys. Rev. B* **65** 235304 (2002); Butov L V et al. *Phys. Rev. Lett.* **87** 216804 (2001)
31. Andreev A F, Lifshits I M *Zh. Eksp. Teor. Fiz.* **56** 2057 (1969) [*Sov. Phys. JETP* **29** 1107 (1969)]; Chester G V *Phys. Rev. A* **2** 256 (1970)
32. Lozovik Yu E, Volkov S Y, Willander M *Pis'ma Zh. Eksp. Teor. Fiz.* **79** 585 (2004) [*JETP Lett.* **79** 473 (2004)]
33. Lozovik Yu E, Nikitkov M V *Zh. Eksp. Teor. Fiz.* **111** 1107 (1997); **116** 1440 (1999) [*JETP* **84** 612 (1997); **89** 775 (1999)]
34. Lozovik Yu E, Semenov A G *Pis'ma Zh. Eksp. Teor. Fiz.* **86** 30 (2007); *Theor. Math. Fiz.* **154** 372 (2008) [*JETP Lett.* **86** 28 (2007)]; *Theor. Math. Phys.* **154** 319 (2008)]; see Lozovik Yu E, Semenov A G, Willander M *Pis'ma Zh. Eksp. Teor. Fiz.* **84** 176 (2006) [*JETP Lett.* **84** 146 (2006)]
35. Voronova N S, Lozovik Yu E *Fiz. Tver. Tela* **50** 1496 (2008) [*Phys. Solid State* **50** 1555 (2008)]
36. Berman O L, Lozovik Yu E, Snoke D W *Phys. Rev. B* **77** 155317 (2008)
37. Deng H et al. *Science* **298** 199 (2002)

PACS numbers: **63.20. - e**, **63.50. - x**, **78.30. - j**
DOI: 10.3367/UFNe.0179.2009031.0313

Inverted optical phonons in ion-covalent crystals

E A Vinogradov, B N Mavrin,
N N Novikova, V A Yakovlev

1. Introduction

In this report, we discuss additional optical phonons, considered excess from the standpoint of selection rules, discovered in the majority of crystals with ion-covalent interatomic bonds, including their solid solutions. These ‘excess’ phonons are located inside the transverse-longitudinal splitting of the main phonons, where the real part of the crystal permittivity is negative, and are split by the crystal field into transverse optical (TO) and longitudinal optical (LO) phonons, the frequencies of ‘excess’ LO phonons turning out to be lower than those of ‘excess’ TO phonons.

Solid solution systems like $\text{Zn}_{1-x}\text{Cd}_x\text{S}$, $\text{Zn}_{1-x}\text{Cd}_x\text{Se}$, and $\text{ZnSe}_x\text{S}_{1-x}$ hold much promise for practical applications, in particular in optoelectronics, due to their unusual physical properties. Structures with quantum wells [1] and quantum dots [2] based on thin layers of these materials, which are candidates for light sources in the blue spectral region, were formed and investigated. Chromium-doped crystals of these materials have proven to show promise for making femtosecond lasers in the near-infrared (IR) region ($\lambda \approx 2.5 - 3.5 \mu\text{m}$) [3, 4].

The compositional disorder of a solid solution modifies the structural, vibrational, and optical properties of polar crystals. These changes give rise to special features in the lattice dynamics of ternary solid solutions of the substitution type (single-mode, two-mode, or intermediate behavior of the transverse ω_{TO} and longitudinal ω_{LO} vibration frequencies of the system [5]) as well as to the emergence of new modes (local, gap, or resonance (quasiresonance) excitations) and to the defect-induced density of phonon states [6].

In the rigid-ion model [7], for a diatomic crystal of the ZnS type, the phonon frequencies ω_{TO} and ω_{LO} are given by [8]

$$\omega_{\text{TO}}^2 = \omega_0^2 - \frac{4\pi}{3} \frac{e_{\text{B}}^2(m_1 + m_2)}{\sigma m_1 m_2}, \quad (1)$$

$$\omega_{\text{LO}}^2 = \omega_0^2 + \frac{8\pi}{3} \frac{e_{\text{B}}^2(m_1 + m_2)}{\sigma m_1 m_2}, \quad (2)$$

$$\omega_0^2 = -\frac{m_1 + m_2}{m_1 m_2} \sum_l \Phi^N \begin{pmatrix} l \\ + - \end{pmatrix}, \quad (3)$$

where m_1 and m_2 are the positive- and negative-ion masses, l is the cell number, σ is the elementary cell volume, ω_0 is the frequency of triply degenerate atomic vibrations, neglecting long-range Coulomb forces, Φ^N are short-range force constants, which are independent of the ion position relative to the crystal surface, and e_{B} is the Born effective charge of an ion. The long-range Coulomb ion field in single crystals partly removes the triple degeneracy of a vibration with the frequency ω_0 , splitting it into a doubly degenerate vibration (ω_{TO}) and a nondegenerate one (ω_{LO}); the symmetry of atomic vibrations remains unaltered in this case.

As follows from formulas (1) and (2), the frequencies of longitudinal optical phonons should always exceed the transverse phonon frequencies:

$$\omega_{LO}^2 - \omega_{TO}^2 = \frac{4\pi e_B^2}{\sigma\mu}, \quad e_B = \frac{\epsilon_\infty + 2}{3} e_S^*, \quad (4)$$

where μ is the reduced dipole mass, ϵ_∞ is the crystal permittivity at frequencies much higher than the phonon frequencies, and e_S^* is the microscopic Szegti charge [9] used to describe the crystal lattice dynamics in the rigid-ion model [7, 8].

This clear and coherent picture is disturbed by the existence of special features in the IR reflection spectra of crystals with ion and ion-covalent atomic bonds. Observed in the majority of such crystals, especially in their ternary solid solutions of the $A_{1-x}B_xC$ type where atoms A and B belong to the same group of the periodic table, are excess (additional with respect to the selection rules) optical phonons at the center of the Brillouin zone with inverted frequencies of the longitudinal ω_{LO}^{add} and transverse optical ω_{TO}^{add} phonons: $\omega_{LO}^{add} < \omega_{TO}^{add}$. In the solid solutions of the polar compounds of the $A_{1-x}B_xC$ type, unlike in the extreme compounds AC and BC , an elementary cell contains not only the base dipoles $A-C$ and $B-C$ but also the $A-B$ dipole, which is an order of magnitude weaker than the base ones [10–18]. Our report is concerned with the investigation of these additional dipoles and their related optical phonons, as well as with an attempt to explain their nature by the example of the monocrystals of $Zn_{1-x}Cd_xS$, $Zn_{1-x}Cd_xSe$, and $ZnSe_xS_{1-x}$ solid solutions.

2. Experiment

The main parameters of the crystal lattice dynamics (the frequencies ω_{TO} and ω_{LO} of optical phonons at the center of the Brillouin zone ($\mathbf{k} \approx 0$), their lifetimes, oscillator strengths, etc.) are derived from the measurements of IR reflection spectra and Raman scattering (RS) spectra [19, 20]. The crystal permittivity, which is related to the majority of the desired parameters, is recovered from the reflection spectrum:

$$\epsilon(\omega) = \epsilon_\infty + \sum_{j=1}^n \frac{4\pi\rho_{TO,j}\omega_{TO,j}^2}{\omega_{TO,j}^2 - \omega^2 - i\gamma_{TO,j}\omega}, \quad (5)$$

where $\omega_{TO,j}$, $4\pi\rho_{TO,j}$, and $\gamma_{TO,j}$ are the frequency, the oscillation strength, and the damping constant of the j th transverse mode and ϵ_∞ is the high-frequency permittivity due to interband electron transitions. In the quasiharmonic approximation, when $\gamma_{TO,j} \ll \omega_{TO,j}$, it is possible to show the validity of the formula [21]

$$\epsilon^{-1}(\omega) = \epsilon_\infty^{-1} - \sum_{j=1}^n \frac{4\pi\rho_{LO,j}\omega_{LO,j}^2}{\omega_{LO,j}^2 - \omega^2 - i\gamma_{LO,j}\omega}, \quad (6)$$

where $\omega_{LO,j}$, $4\pi\rho_{LO,j}$, and $\gamma_{LO,j}$ are the frequencies, the oscillation strengths, and the damping constants of the longitudinal optical vibrations (phonons).

The spectral dependences of $\text{Im } \epsilon(\omega)$ and $\text{Im } (-\epsilon^{-1}(\omega))$ with $\epsilon(\omega)$ in the form of expressions (5) and (6) each have j peaks at the respective frequencies $\omega_{TO,j}$ and $\omega_{LO,j}$. The width of each peak is equal to the corresponding damping constant: $\gamma_{TO,j}$ or $\gamma_{LO,j}$. In this case, the oscillator strengths of the transverse and longitudinal vibration modes, under the condition that their damping is weak and $\gamma_{TO,j}$,

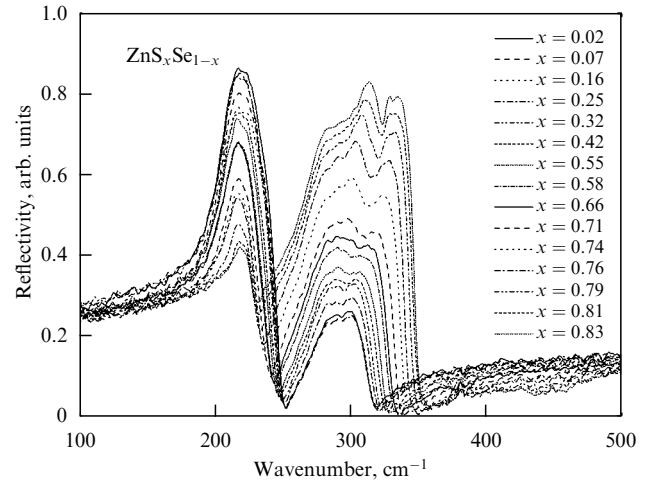


Figure 1. Reflection spectra of a family of $ZnSe_xS_{1-x}$ crystals for a near-normal incidence of radiation [17].

$\gamma_{LO,j} \ll \omega_{TO,j}$, are expressed by the formulas [20]

$$4\pi\rho_{TO,j} = \frac{\gamma_{TO,j}}{\omega_{TO,j}} \text{Im } \epsilon(\omega_{TO,j}), \quad (7)$$

$$4\pi\rho_{LO,j} = \frac{\gamma_{LO,j}}{\omega_{LO,j}} \text{Im } (-\epsilon^{-1}(\omega_{LO,j})). \quad (8)$$

The crystal permittivity $\epsilon(\omega)$ may be recovered from the experimental reflection spectrum $R(\omega)$ by means of the integral Kramers–Kronig relations. The parameters ϵ_∞ , $\omega_{TO,j}$, $4\pi\rho_{TO,j}$, and $\gamma_{TO,j}$ may be determined from the measured reflection spectrum of a specimen by selecting them in such a way as to minimize the misfit between the calculated reflection spectrum and the measured one.

For example, Fig. 1 shows the reflection spectra of a family of $ZnSe_xS_{1-x}$ crystals. A feature in the form of a small dip is observed in the high-frequency band of the residual rays (in the ZnS-like modes). In the frequency range between the frequencies ω_{TO} and ω_{LO} of the ZnS-like modes, two additional modes were discovered, one of which ($\sim 300 \text{ cm}^{-1}$), well visible in the spectra of RS and enhanced due to a Fermi resonance, is attributed to the second-order line, and the other (near 325 cm^{-1}) is attributed to the quasiresonance mode of the atomic Se impurity in ZnS for small x [16, 17].

Figure 2 shows the optical phonon frequencies recovered from IR reflection spectra [16, 17]. The dependence of the ZnS- and ZnSe-like TO and LO modes on the composition of solid solutions is unambiguously interpreted as the double-mode behavior of optical phonons and is in good agreement with the results of previous investigations of optical phonons in $ZnSe_xS_{1-x}$. The additional mode at a frequency close to 325 cm^{-1} has an inverted TO–LO doublet. To verify the possibility that such an impurity vibrational mode exists, the vibration frequencies of an atomic Se impurity in a ZnS crystal were calculated based on the microscopic dynamic theory of a crystal lattice with a low impurity density, developed in [22].

3. Discussion

The vibration frequencies of impurity atoms (in the mass defect approximation) are rather well described by Vinogra-

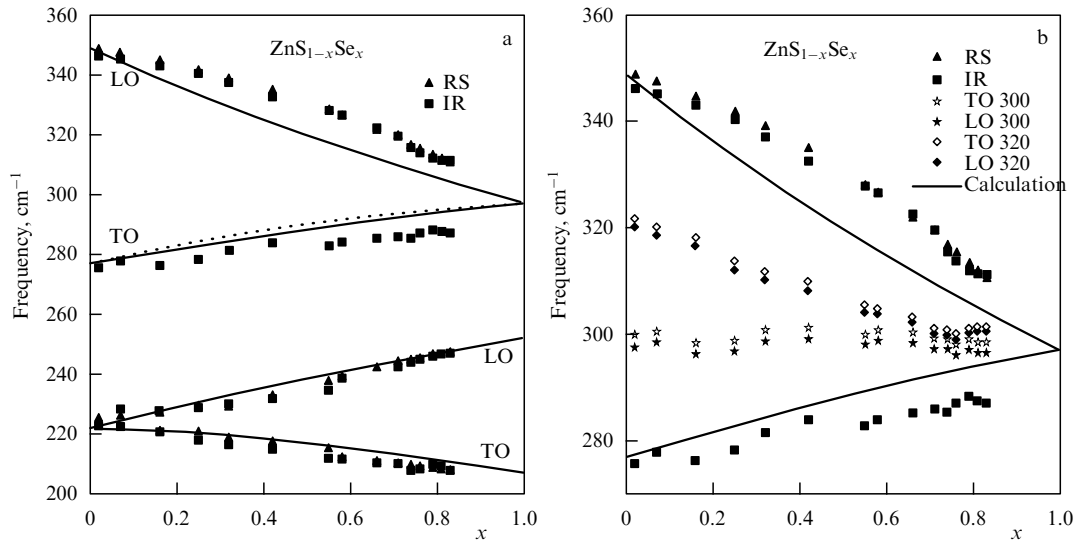


Figure 2. Density dependence of the optical phonon frequencies of $\text{ZnS}_{1-x}\text{Se}_x$ single crystals derived from IR reflection and RS spectra [16, 17]: (a) main ZnS- and ZnSe-like optical phonons, (b) additional optical phonons inside the LO–TO splitting of the main ZnS-like phonons; between them are two branches of inverted phonons, which converge to the local vibration frequency of sulfur atoms in ZnSe.

dov's theory [22] at densities $x < 0.3$ and $1 - x < 0.3$ [9–13, 18] if the optical phonon density-of-state function and the atomic vibration amplitudes of the impurity-free crystal are known. As shown in Ref. [13], in the system of solid solution $\text{Zn}_{1-x}\text{Cd}_x\text{S}$, calculations based on the theory in [22] with the use of the phonon density-of-state function in ZnS from Ref. [23] described the experimental data in Ref. [12] unexpectedly well, without recourse to fitting parameters, throughout the density range, including the frequencies of additional (inverted) phonons. Additional phonons in $\text{Zn}_{1-x}\text{Cd}_x\text{S}$ were attributed to the quasilocal vibrations of Cd atoms in ZnS. These quasilocal vibrations fall within the quasigap in the optical phonon density of states of ZnS [23].

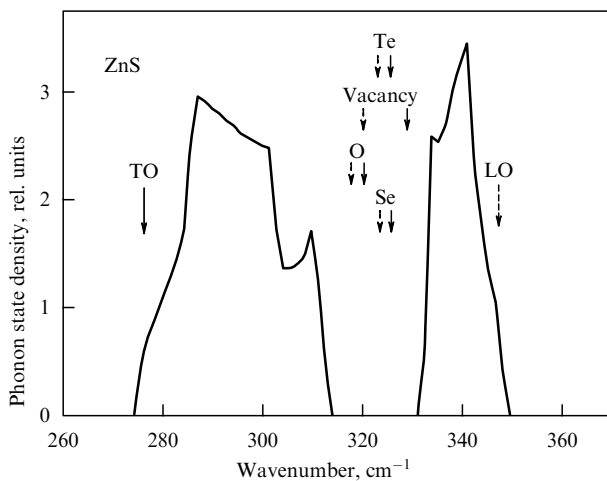


Figure 3. Density of optical phonon states for a cubic ZnS monocystal [23]. The optical phonon frequencies are $\omega_{\text{TO}} = 276 \text{ cm}^{-1}$ and $\omega_{\text{LO}} = 350 \text{ cm}^{-1}$. The vibration frequencies of impurity atoms that replace sulfur atoms, as well as the vibration frequencies of atomic sulfur vacancies, which fall within the quasigap in the density of optical phonon states, are indicated by arrows: solid arrows correspond to transverse vibrations and dashed arrows correspond to the longitudinal vibrations of impurity atoms with a density of 20%.

Figure 3 shows the results of a solution of Vinogradov's equation for impurity atoms of a mass m^* , which replace sulfur atoms in ZnS, with $m^* = 0$ (a sulfur vacancy), $m^* = 16$ (oxygen), $m^* = 79$ (selenium), and $m^* = 127.6$ (tellurium).

An analysis of the known data on the phonon dispersion and phonon density-of-state function in ion-covalent crystals showed that the optical phonon density of states has a dip at frequencies between the LO and TO phonons at the center of the Brillouin zone for virtually all crystals of A^1B^7 and A^2B^6 compounds, as well as for several A^3B^5 crystals. In ZnS, this dip (quasigap), as it were, divides the density of optical phonon states into two parts: transverse optical phonons prevail in the low-frequency part and the longitudinal ones prevail in the high-frequency part. As follows from formula (4), the magnitude of the LO–TO splitting at the center of the Brillouin zone is proportional to the square of the ion charge. The higher the degree of ionicity of a compound, the greater is this splitting. The results of calculation of the optical phonon dispersion throughout the Brillouin zone [23] suggest that the LO–TO splitting at the center of the Brillouin zone may be comparable to (or even exceed) the dispersion of optical phonons over the Brillouin zone for many ionic and ion-covalent crystals, giving rise to a quasigap in the density of optical phonon states.

As follows from formula (4), experimental data allow determining the value of the effective microscopic ion charge e_s^* , which was previously measured for A^2B^6 compounds with an uncertainty of $\pm 0.02e$ [24]: $e_s^*(\text{ZnS}) = 0.88e$; $e_s^*(\text{ZnSe}) = 0.72e$; $e_s^*(\text{ZnTe}) = 0.65e$; $e_s^*(\text{CdS}) = 0.87e$; $e_s^*(\text{CdSe}) = 0.83e$; $e_s^*(\text{CdTe}) = 0.74e$. For a $\text{ZnSe}_x\text{S}_{1-x}$ alloy, in particular, the difference in the charges of sulfur and selenium ions on substitution of selenium for sulfur atoms is equal to 0.16 of the electron charge. This implies that for a total electroneutrality of a cell of the solid solution crystal, there must be an S–Se dipole with the oscillator strength 10 times lower than for the Zn–S and Zn–Se dipoles, because its charges amount to $\pm 0.08e$ rather than to about $\pm 0.8e$ as in the extreme compounds. Jahne [18] hypothesized that in the solid solutions of $A_{1-x}B_xC$ com-

pounds, unlike in the binary extreme compounds AC and BC , an A^2B^6 dipole may be present in an elementary cell along with the $A-C$ and $B-C$ dipoles. As is clear from the experimental values of the ion charges of $A-B$ compounds outlined above, an $S-Se$ dipole may exist in the solid solution $ZnSe_xS_{1-x}$.

In the system of $Zn_{1-x}Cd_xSe$ solid solutions, additional inverted phonons were also discovered in the frequency range where the real part of the crystal permittivity is negative: between the principal frequencies of TO and LO phonons [14]. In Ref. [14], the normal vibrations of atoms were also found theoretically in the framework of the isodisplacement model [18, 25], which takes the interaction of $ZnSe$ - and $CdSe$ -like vibrations into account. The main assumption underlying this model is that the anions and cations of the $ZnSe$ ($CdSe$) groups oscillate in phase with the same amplitude and that every ion experiences forces statistically averaged over all its neighbors. Calculated for $Zn_{1-x}Cd_xSe$ were the density dependences of the optical mode frequencies and oscillator strengths, which were seen to agree with the experimental ones quite well. The amplitudes of atomic displacements were also calculated. It was shown that apart from vibrations related to the $Zn-Se$ and $Cd-Se$ dipoles, there are vibrations under which Se atoms are virtually immobile, while Zn and Cd atoms oscillate relative to each other to make up a weak $Zn-Cd$ dipole.

For $x = 0$, Zn and Se atoms in the principal mode vibrate in antiphase, which is well known for the optical mode in the $ZnSe$ crystal. With increasing x , Cd atoms begin to participate in this vibration, to oscillate in phase with Zn atoms, and their amplitude increases, while the amplitude of atomic Zn vibrations decreases. In this case, the amplitude of atomic Se vibrations depends on the solid solution composition only slightly.

In the quasiresonance mode with inverted LO and TO phonon frequencies, Cd and Zn atoms vibrate in antiphase, while Se atoms are hardly involved in this mode [14]. With increasing x , the amplitude of atomic Cd displacements decreases, but the displacement amplitude of Zn atoms, which vibrate in antiphase to Cd atoms, increases. The dipole moment emerging in these vibrations is defined by the difference between the atomic charges of Zn and Cd ions. This difference is moderate, and the dipole moment of the $Zn-Cd$ vibrations is nearly 10 times smaller than the dipole moment of the principal modes ($Zn-Se$ or $Cd-Se$). This implies the low oscillator strengths of the $Zn-Cd$ vibrations and the low magnitudes of the RS peaks and the functions $Im\epsilon(\omega)$ and $Im(-\epsilon^{-1}(\omega))$ for the $Zn-Cd$ mode [14, 15].

4. Summary

Because of the different degrees of ionicity of binary solution pairs (the difference in Szigeti charges), there emerge additional weak $Zn-Cd$ dipoles related to relative ion vibrations in the solid solutions $Zn_{1-x}Cd_xS$, $Zn_{1-x}Cd_xSe$, and $Zn_{1-x}Cd_xTe$, and weak $S-Se$ dipoles in $ZnSe_xS_{1-x}$. In the binary solid solutions of $A_{1-x}B_xC$ compounds, unlike in the extreme binary compounds AC and BC , an elementary cell contains not only the base dipoles $A-C$ and $B-C$ but also the $A-B$ dipole, which is an order of magnitude weaker than the base ones. This removes the contradiction related to the initially apparent violation of selection rules.

Additional inverted phonons emerge due to the high degree of ionicity of A^2B^6 compounds, and the magnitude of the transverse-longitudinal splitting of phonons at the center of the Brillouin zone turns out to be sufficiently large in comparison with the phonon dispersion over the entire Brillouin zone. That is why a quasigap, within which the vibrations of impurity atoms fall, emerges in the density of optical phonon states. The vibrations of impurity atoms in the quasigap should be considered quasilocal or quasiresonance, depending on the parameters of the quasigap (its width and depth). In the quasigap region, the real part of the crystal permittivity is negative: the transverse-longitudinal splitting of the quasilocal or quasigap vibrations of impurity atoms turns out to be inverted, i.e., the longitudinal vibrations of impurity atoms are lower in frequency than the transverse ones.

We also note that IR reflection spectra are always recorded from the crystal surface, and the surface layer typically contains numerous stacking faults like vacancies, changes in interatomic distances, and other defects arising from contamination of the crystal surface by adsorbed atoms and molecules. It can be seen from Fig. 3 that the vibration of vacancies may fall within the quasigap in the density of optical phonon states to produce the spectral reflectivity feature under discussion.

References

1. Giugno P et al. *Phys. Rev. B* **54** 16934 (1996)
2. Gasser C et al. *Appl. Phys. Lett.* **72** 972 (1998)
3. Sorokin E, Naumov S, Sorokina I T *IEEE J. Selected Topics Quantum Electron.* **11** 690 (2005)
4. Sorokina I T et al. *OSA Trends Optics Photonics* **98** 263 (2005)
5. Genzel L, Martin T P, Perry C H *Phys. Status Solidi B* **62** 83 (1974)
6. Hayes W, Loudon R *Scattering of Light by Crystals* (New York: Wiley, 1978)
7. Kellermann E W *Philos. Trans. R. Soc. London A* **238** 513 (1940)
8. Balkanski M, in *Proc. Intern. Conf. on II-VI Semiconducting Compounds* (Rhode Islands: Flammation, 1963) p. 1007
9. Szigeti B *Trans. Faraday Soc.* **45** 155 (1949)
10. Vodop'yanov L K, Vinogradov E A, Vinogradov V S *Fiz. Tverd. Tela* **16** 849 (1974) [*Sov. Phys. Solid State* **16** 545 (1974)]
11. Vodopyanov L K, Vinogradov E A *Cryst. Lattice Defects* **5** 125 (1974)
12. Mityagin Yu A, Vodop'yanov L K, Vinogradov E A *Fiz. Tverd. Tela* **17** 2054 (1975) [*Sov. Phys. Solid State* **17** 1341 (1975)]
13. Vinogradov E A, Mityagin Yu A *Fiz. Tverd. Tela* **20** 3162 (1978) [*Sov. Phys. Solid State* **20** 1825 (1978)]
14. Vinogradov E A, Mavrin B N, Vodop'yanov L K *Zh. Eksp. Teor. Fiz.* **126** 866 (2004) [*JETP* **99** 749 (2004)]
15. Vodopyanov L K et al. *Phys. Status Solidi C* **1** 3162 (2004)
16. Vinogradov E A, Mavrin B N, Novikova N N, Yakovlev V A *Fiz. Tverd. Tela* **48** 1826 (2006) [*Phys. Solid State* **48** 1940 (2006)]
17. Vinogradov E A et al. *Laser Phys.* **19** (2) 162 (2009)
18. Jahne E *Phys. Status Solidi B* **74** 275 (1976); **75** 221 (1976)
19. Born M, Huang Kun *Dynamic Theory of Crystal Lattices* (Oxford: Clarendon Press, 1954) [Translated into Russian (Moscow: IL, 1958)]
20. Vinogradov E A, Khammatov I I *Spektroskopiya Ob"emnykh i Poverkhnostnykh Fononov Kristallov* (Spectroscopy of Bulk and Surface Phonons in Crystals) (Tashkent: FAN, 1989)
21. Belousov M V *Fiz. Tverd. Tela* **15** 1206 (1973) [*Sov. Phys. Solid State* **15** 813 (1973)]
22. Vinogradov V S *Fiz. Tverd. Tela* **11** 2062 (1969) [*Sov. Phys. Solid State* **11** 1666 (1969)]
23. Bilz H, Kress W *Phonon Dispersion Relations in Insulators* (Berlin: Springer-Verlag, 1979)
24. Vinogradov E A, Author's Abstract of Thesis for Candidate's Degree (Dolgoprudnyi: MFTI, 1973)
25. Peterson D L et al. *Phys. Rev. B* **33** 1160 (1986)